

Beam-beam detuning formula and its agreement with MadX. Individual collisions.

TRI-BN 2214

Dobrin Kaltchev

ARTICLE HISTORY
Compiled May 24, 2022

1. Introduction

The goal is to compute the horizontal and vertical amplitude-dependant detunings $\Delta Q_{x,y}$ generated by a general (head-on or long-range, round or flat) beam-beam collision and compare the result with MadX. The formulae are the same as in a previous report [1]. Some more recent development can be found in [2] (not yet published, link to be added). An implementation as *Mathematica* scripts is also included. In the examples, these scripts are used to reproduce results similar to the ones in [1], this time for a latest HL-LHC lattice and beam-beam setup (round-beam optics).

The collision is described by two parameters:

- (1) one of either d_x or d_y – full separation between orbits normalized to corresponding strong-beam rms size σ_x or σ_y (for the LHC, only one of $d_{x,y}$ can be non-zero);
- (2) $r = \sigma_y/\sigma_x$ – sigma-aspect ratio of the strong beam.

The analytic expressions for $\Delta Q_{x,y}$ should agree with the detunings found with MadX. These are denoted with Δ TUNX, Δ TUNY and defined as the TUNX, TUNY columns in the tracking output file `dynaptune` with subtracted the detuning in absence of beam-beam. The latter is a contribution of other sources (octupoles etc) and is found in a separate (preceding) run of MadX. Numerical errors may also interfere.

Same as in [1], some small residual detuning that depends on the crossing angle may be present: see [1] (page 3): “For each plot, before the comparison is made, tiny tune shifts $\sim 5 \times 10^{-5}$ still present in the beam-beam free lattice are subtracted from the MadX output”.

For section Results, by choosing a set of weak-beam particle amplitudes a_x, a_y , such as the one on Fig 1 (up to 7σ), the analytic footprint $\Delta Q_{x,y}(a_x, a_y)$ is plotted together with the one from tracking.

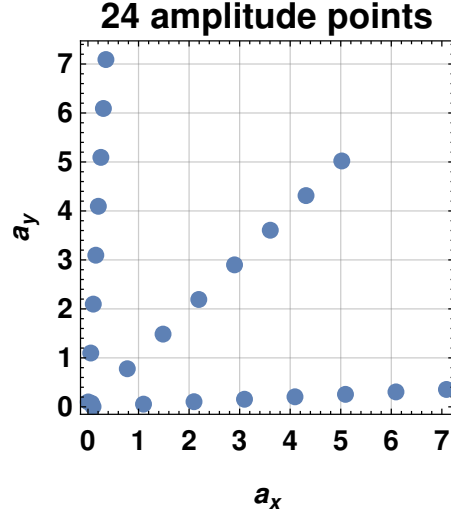


Figure 1. Sample range of weak-beam particle amplitudes.

2. Theory

- An expression for the averaged Hamiltonian, the Fourier coefficient C_{mk} for $k = m = 0$, can be found in [2], Eqn (2.6), or in [1], Eqn 10 (top):

$$C_{00} = \int_0^1 \frac{dt}{t g_r(t)} \left[1 - \mathbf{Q}_0^{(x)}(t) \mathbf{Q}_0^{(y)}(t) \right].$$

Here $\mathbf{Q}_0^{(x)}(t), \mathbf{Q}_0^{(y)}(t)$ depend on the location of the collision ($d_{x,(y)}, r$) and amplitudes (a_x, a_y) see the Introduction. In fact the above dependence realises through some mixed location-amplitudes variables, also called "bar" variables in [2], see Eqn 2.8.

- The derivatives over $a_{x,y}$, [1], are

$$\begin{aligned} \frac{\partial C_{00}}{\partial a_x} &= - \int_0^1 \frac{dt}{t g_r(t)} \frac{\partial \mathbf{Q}_0^{(x)}(t)}{\partial a_x} \mathbf{Q}_0^{(y)}(t) \\ \frac{\partial C_{00}}{\partial a_y} &= - \int_0^1 \frac{dt}{t g_r(t)} \frac{\partial \mathbf{Q}_0^{(y)}(t)}{\partial a_y} \mathbf{Q}_0^{(x)}(t). \end{aligned} \quad (2.1)$$

- It is further shown in [1] that the derivatives of $\mathbf{Q}_0^{(x)}(t), \mathbf{Q}_0^{(y)}(t)$ participating in Eqn 2.1 can be expressed in terms of the first three 2D-Bessel functions $\Lambda_{0,1,2}$, see Eqn 1.2 in [2].

Namely, since

$$\mathbf{Q}_0^{(z)} = e^{-\frac{t}{2}(\bar{a}_z - \bar{d}_z)^2} \Lambda_0$$

($z = x, y$) one can after some transformations show that

$$\begin{aligned} \frac{\partial \mathbf{Q}_0^{(z)}}{\partial a_z} &= \eta_z(r, t) e^{-\frac{i}{2}(\bar{a}_z - \bar{d}_z)^2} \left[-\frac{\bar{a}_z}{2} [\Lambda_0 + \Lambda_2] + \bar{d}_z \Lambda_1 \right] \\ \eta_x(r, t) &\equiv rt, \quad \eta_y(r, t) \equiv t/g_r(t). \end{aligned} \quad (2.2)$$

- Sufficiently far from the strong-beam core, approximately when $|a_x| < 5$, see Figure 1, the generalized two-dimensional Bessel function can be defined with the sums:

$$\Lambda_n(X, Y) = e^{-X-Y} \sum_{q=-q_{\max}}^{q_{\max}} I_{n-2q}(X) I_q(Y), \quad (2.3)$$

where $I_q(u)$ is the modified Bessel functions of the first kind. For large normalized separations and amplitudes, large q_{\max} is needed ~ 30 , see also [3]. For large separations and amplitudes close to the strong beam core, the form as complex integral must be used as the above sum diverges. The following (real) integral follows from the generating function of 2D-Bessel:

$$\Lambda_n(X, Y) = \frac{i^{-n}}{2\pi} e^{-X-2Y} \int_0^{2\pi} e^{-in\phi - X \sin\phi + 2Y \sin^2\phi} d\phi. \quad (2.4)$$

- The flatness-parameter appearing under the integral Eqn 2.1 is a function of t and r :

$$g_r(t) \equiv \sqrt{1 + (r^2 - 1)t}. \quad (2.5)$$

- The analytic detunings finally are

$$\Delta Q_z = \frac{2\xi}{a_z} \frac{\partial C_{00}}{\partial a_z}, \quad \text{where } z = x \text{ or } y \quad (2.6)$$

and $\xi \equiv \frac{N_b r_0}{4\pi\gamma\epsilon}$ is the beam-beam parameter.

3. Mathematica implementation

Notebook download: [tri-dn-analytic-footprint.nb](#)

- Let $a_{x,y}$ and $d_{x,y}$ be encoded as ax, ay, dx, dy and let also $\xi = \xi$. Then

Code Mathematica 1 for Eqn 2.6

```

1 | dQxy[{ax_, ay_}] :=
2 |   - 2 xi {
3 |     DXC00[dx, dy, r, ax, ay]/ax
4 |     ,
5 |     DYC00[dx, dy, r, ax, ay]/ay
6 |   };

```

Note that with Mathematica, $\{a, b\}$ describes the two-dimensional vector (a, b) .

- the 2D-Bessel function

Code Mathematica 2 for Eqn 2.3

```

1 | Bess2D[X_, Y_, n_] := Sum[
2 |   Exp[-X] BesselI[n-2q, X]
3 |   Exp[-Y] BesselI[q, Y]
4 |   , {q, -qmax, qmax}]

```

- The flatness-parameter

Code Mathematica 3 for Eqn 2.5

```

1 | g[t_, r_] := Sqrt[1 + (r^2 - 1) t];

```

- The analytic detunings Eqn 2.6 depend only on the two derivatives, Eqn 2.1. These are implemented in *Mathematica* as the following functions DXC00 and DYC00.

For both scripts shown on the next two pages lines 3-10 are identical and perform the same transform to bar variables. Note that the script describing DYC00 is nearly exactly the same as the one for DXC00. It differs only in line 12 and lines 16–17 (obtained by simply replacing x with y).

Code Mathematica 4 for Eqns 2.1

```
1 DXC00[dx_, dy_, r_, ax_, ay_] := Module[{},
2   -NIntegrate[
3     axbar = ax r;
4     aybar = ay /g[t, r];
5     dxbar = dx;
6     dybar = dy r/g[t, r];
7     U1x = axbar dxbar ;
8     U2x = - 1/4 axbar^2 ;
9     U1y = aybar dybar ;
10    U2y = - 1/4 aybar^2;
11
12    r/g[t, r]
13    Exp[(-t/2 ((axbar - dxbar)^2 + (aybar - dybar)^2))]
14    Bess2D[U1y t, U2y t, 0]
15    (
16    -axbar/2 (Bess2D[U1x t, U2x t, 0] + Bess2D[U1x t, U2x t, 2])
17    + dxbar Bess2D[U1x t, U2x t, 1]
18    )
19    , {t, 0, 1}]
20  ]
```

Code Mathematica 5 Eqns 2.1 continued

```
1 DYCOO[dx_, dy_, r_, ax_, ay_] := Module[{},
2   -NIntegrate[
3     axbar = ax r;
4     aybar = ay /g[t, r];
5     dxbar = dx;
6     dybar = dy r/g[t, r];
7     U1x = axbar dxbar ;
8     U2x = - 1/4 axbar^2 ;
9     U1y = aybar dybar ;
10    U2y = - 1/4 aybar^2;
11
12    1/g[t, r]^2
13    Exp[(-t/2 ((axbar - dxbar)^2 + (aybar - dybar)^2))]
14    Bess2D[U1x t, U2x t, 0]
15    (
16    -aybar/2 (Bess2D[U1y t, U2y t, 0] + Bess2D[U1y t, U2y t, 2])
17    + dybar Bess2D[U1y t, U2y t, 1]
18    )
19    , {t, 0, 1}]
20  ]
```

4. Results

4.1. Long range, round or flat

A flat l.r.is one for which $r \neq 1$.

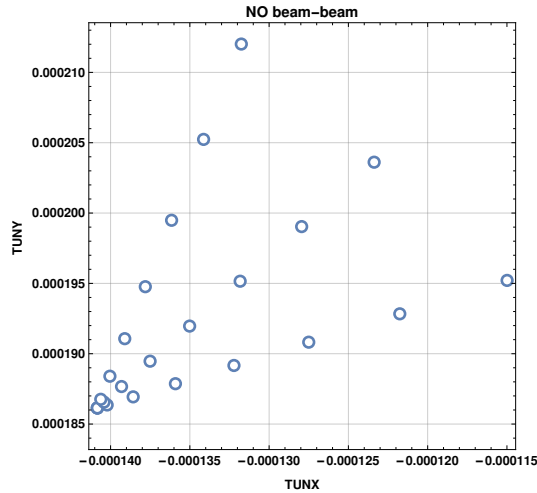


Figure 2. Small residual detuning in absence of beam-beam (MadX), see Introduction and [1]. Half crossing angle = 250 μ rad, Sextupoles and octupoles are off, $\Delta p/p = 0$. It is most likely caused by the off-axis orbit excursion within the IR quadrupoles (comment of Guido Sterbini).

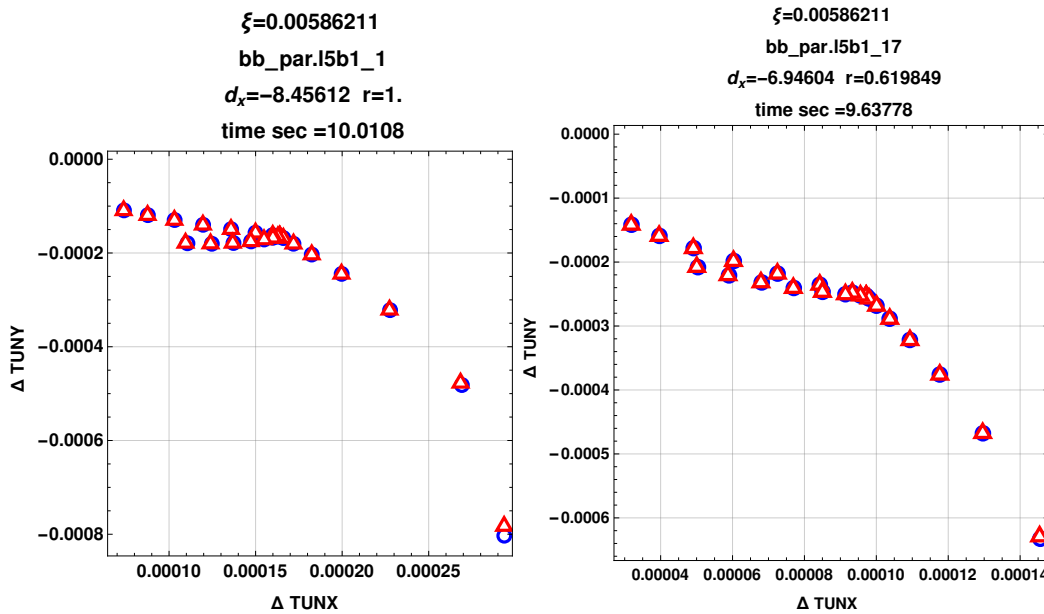


Figure 3. Comparisons of $\Delta TUNX$, $\Delta TUNY$ (blue circles) and $\Delta Q_{x,y}$ Eqn 2.6 (red triangles)

4.2. Behaviour near the strong beam core

Figure 4 shows an example for a case where weak-beam particles with $a_x \sim 6 - 7$ are too close to the strong-beam core and hence the sum in Eqn 2.3 diverges. Choosing a higher $q_{\max} > 20$ does not cure this problem. Here the long-range collision is 12-Left with $d_x = -12.4$. Since the quantity $7 + 12 \sim 19$ is too large, the complex representation of 2D-Bessel Eqn 2.4 has been used. The computing time is 20 times larger than the one for the sum formula.

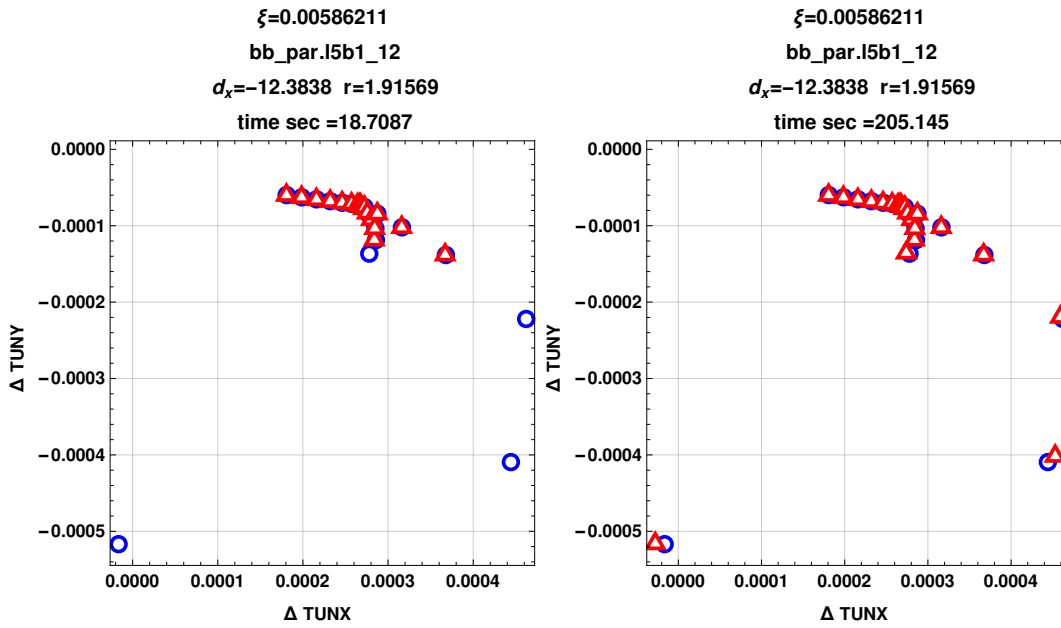


Figure 4. Left: The sum representation of 2D-Bessel Eqn 2.3. Right: The integral Eqn 2.4.

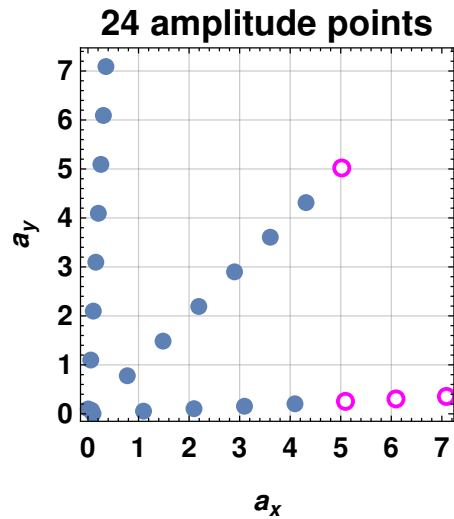


Figure 5. Identification of the divergent amplitudes near the strong-beam core (magenta circles). For these the sum Eqn 2.3 becomes infinity and the complex representation of 2D-Bessel Eqn 2.4 is needed

4.3. Other examples

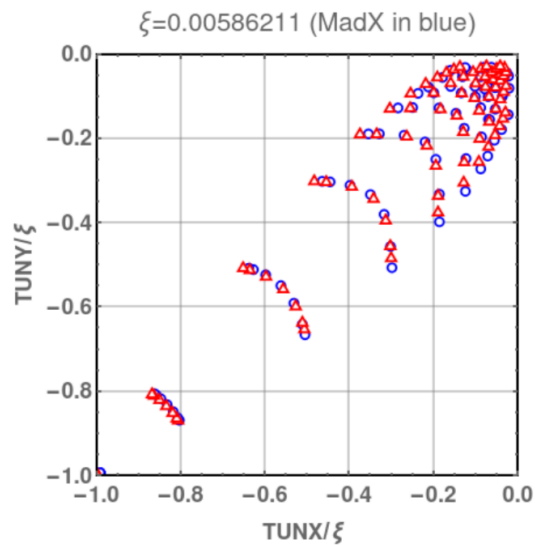


Figure 6. Head-on IP5.

References

- [1] D. Kaltchev, *Fourier Coefficients of Long-Range Beam-Beam Hamiltonian via Two-Dimensional Bessel functions* Proc. of IPAC 2018, Vancouver BC, Canada

- [2] D.Kaltchev *Beam-beam resonance driving terms via Two-dimensional Bessel functions with applications to wire correction in the HL-LHC* (in preparation)
- [3] Y. Papaphilippou, F. Zimmermann, *Estimates of diffusion due to long-range beam-beam collisions*, Phys Rev ST, Volume 5, 074001 (2002)